Electronic Supplementary Material (ESI) for Soft Matter

Electronic Supporting Information

Self-organization of the bacterial cell-division protein FtsZ in confined environments

Sonia Mellouli,[a]* Begoña Monterroso,[b]* Hanumantha Rao Vutukuri,[a] Esra te Brinke,[a] Venkatachalam Chokkalingam,[a] Germán Rivas[b] and Wilhelm T. S. Huck[a]

* these authors contributed equally

[a] Institute for Molecules and Materials, Radboud University Nijmegen, Heyendaalseweg 135, 6525 AJ Nijmegen, The Netherland. E-mail: w.huck@science.ru.nl
[b] Centro de Investigaciones Biológicas, CSIC, Ramiro de Maeztu 9, E-28040 Madrid, Spain. E-mail: grivas@cib.csic.es

Figure S1. Microfluidic chip fabrication by photolithography

Figure S2. Microfluidic chip design

Figure S3. Bulk emulsion of FtsZ bundles in Squalane containing different lipid surfactants

Figure S4. Bulk emulsion of FtsZ bundles in different oil containing *E. coli* lipids (25 g L^{-1})

Figure S5. FRAP experiment

Figure S6. Arrangement of FtsZ bundles in droplets containing 150 g L^{-1} Ficoll and different FtsZ concentrations

Figure S1. Microfluidic chip fabrication by photolithography

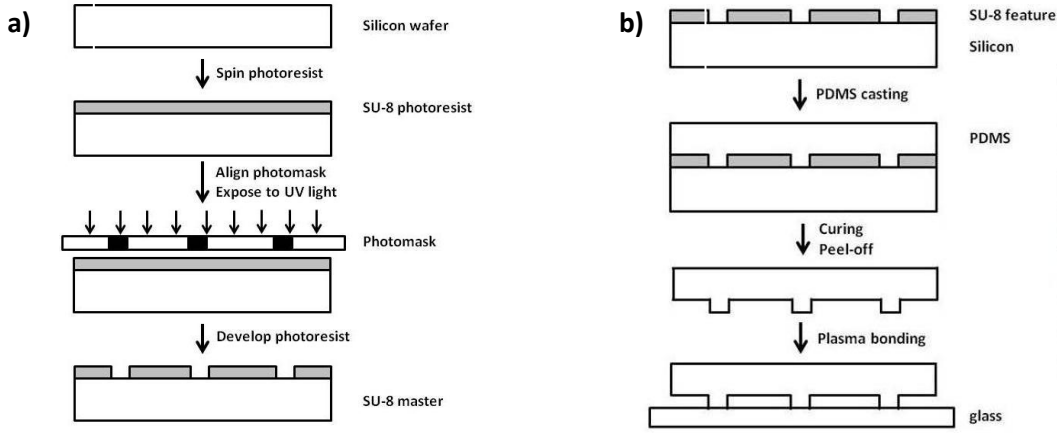

In order to fabricate microchannels, photolithographic fabrication was employed. SU-8 negative photoresist (Micro Resist Technology GmbH, Germany) was used for fabrication purposes. The device fabrication (scheme a) started with creating a design in an AutoCAD program. A high resolution commercial image setter then printed this design on a transparency (JD Photo tools, UK). This transparency served as the photomask in contact photolithography to produce a negative relief in photoresist on a glass substrate. SU8-2025 photoresist is spin coated on a round Silicon wafer with 50 mm diameter (Si-Mat silicon materials, Germany). Spin coating parameters were optimized to achieve the desired film thickness. Subsequently, the sample was soft baked for 1 min at 65°C, 3 min at 95°C and 1 min at 65°C in order to evaporate the solvent and densify the film. Then, the samples were exposed to UV light (λ = 365 nm) in the mask aligner (Karl Suss MJB 3 UV 300/400) for 28 seconds through the photomask. After exposure, the sample was post-baked for a time which depended on the thickness of the photoresist (1 min at 65°C, 2 min at 95°C and 1 min at 65°C). The samples were rinsed with developer solution (mr-Dev600, Micro Resist Technology GmbH, Germany) to remove the non-crosslinked regions. Thus the fabrication of the SU-8 mask was accomplished on a silicon wafer which resulted in 28 micron height channels. In order to achieve 10 micron height channels, SU8-2007 photo resist was used with an exposure time of 20 seconds. This master is used as a mold for soft-lithographic technique to have PDMS channels. The main steps in PDMS device fabrication are sketched in scheme b. PDMS base Sylgard™ 184 and curing agent (Dow Corning GmbH, Germany) were mixed in a ratio of 10:1 w/w, degassed and decanted onto the SU-8 master. Once mixed, poured over the master and heated to elevated temperatures, the liquid mixture becomes a solid, cross-linked elastomer in a few hours via the hydrosilylation reaction between vinyl groups ($SiCH{=}CH_2$) and hydrosilane groups (SiH). After thermal curing for 2-3 hours in an oven at 65°C, PDMS facilitates easy peeling from the SU-8 master. In order to use these PDMS structures as microfluidic devices, inlet holes were punched and the channels were sealed by a glass slide. Surface activation by oxygen plasma (Diener electronic GmbH, Germany) was used for PDMS-glass bonding.

Figure S2. Schematic illustration of the microfluidic chip design

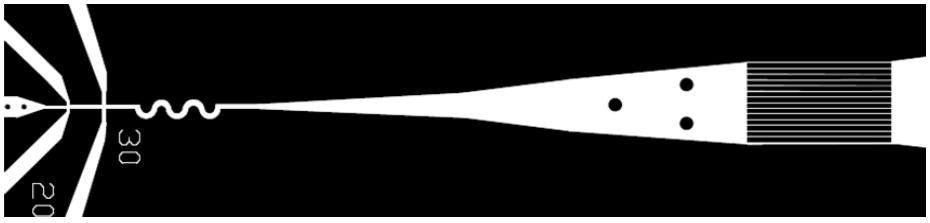

Schematic overview of our microchip used for droplet production. Two streams of dispersed aqueous phases are mixed prior to the droplet formation junction. One stream contains FtsZ at a certain concentration, the other stream delivers GTP at a concentration of 6mM. Automated syringe pumps controlled the flow rates inside the microfluidic device and uniform droplet production (20 pL; coefficient of variance < 0.9%) at a production frequency of around 300 droplets/sec. The narrow channels in the reservoir (~20 µm width and 800 µm long) were meant to study FtsZ behaviour in cylinder shape droplets but fast drying of the droplets when trapped in the channels impaired analysis. Therefore, we focused only on 3D (spherical) and 2D (disc-shaped) droplets using devices of different height (28 µm and 10 µm).

Figure S3. Bulk emulsion of FtsZ bundles in squalane containing different lipids (25 g L^{-1})

Bulk emulsions were prepared by gently pipetting up and down two immiscible solutions: an aqueous phase containing 0.5 g L^{-1} FtsZ, 100 g L^{-1} Ficoll, 1mM GTP in working buffer (50 mM Tris-HCl, pH 7.5, 500 mM KCl, 5 mM $MgCl_2$) and an oil phase composed of the specified lipids dissolved in oil.

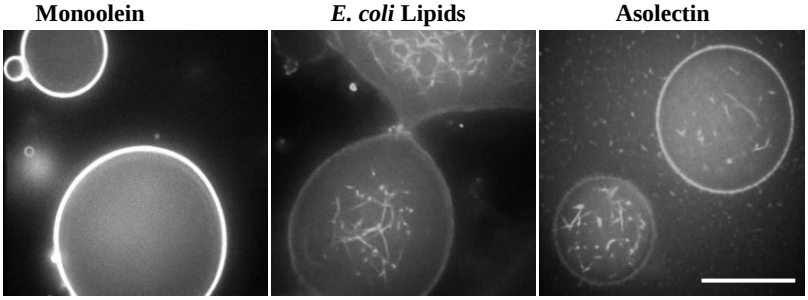

FtsZ bundles were only observed with asolectin and *E. coli* lipids. With monoolein as a surfactant, the high fluorescence intensity at the droplet surface shows that most of FtsZ is adsorbed at the surface explaining the absence of FtsZ bundles in the droplet. Scale bar = 20 µm

Figure S4. Bulk emulsion of FtsZ bundles in different oil phases containing *E. coli* lipids (25 g L^{-1})

Bulk emulsions prepared as in Fig. S3.

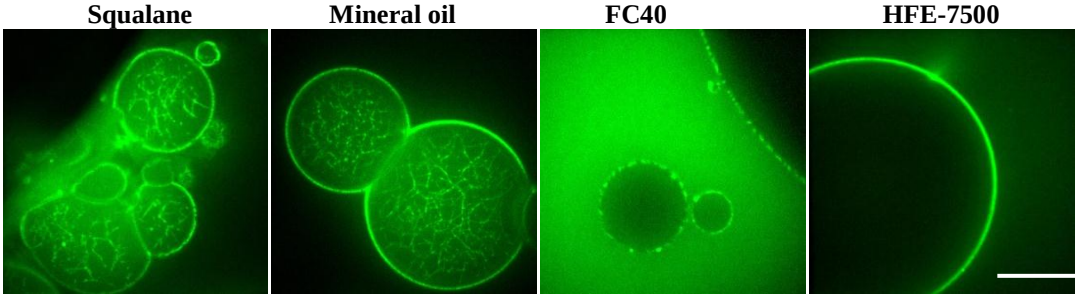

No FtsZ bundles are observed in droplets surrounded by fluorinated oils: HFE-7500 or FC40. In the case of HFE, all FtsZ appeared attached to the surface, probably as a result of improper formation of the lipid monolayer at the oil-water interface. With FC40, the presence of protein in the oil phase might be reflecting an even poorer ability of the *E. coli* lipids to properly form the monolayer. It cannot be discarded some kind of unspecific interaction with FtsZ, as no bundles are observed. With squalane, distribution of FtsZ bundles within droplets is not homogeneous and some aggregates are visible around the droplets. Finally, in mineral oil, FtsZ bundles are nicely distributed in the droplets, while no aggregates and almost no fluorescent intensity is observed in the oil phase. *E. coli* in mineral oil seems to be the best combination of oil-surfactant for the observation of FtsZ bundles in droplets. Scale bar = 20 µm

Figure S5. FRAP experiments

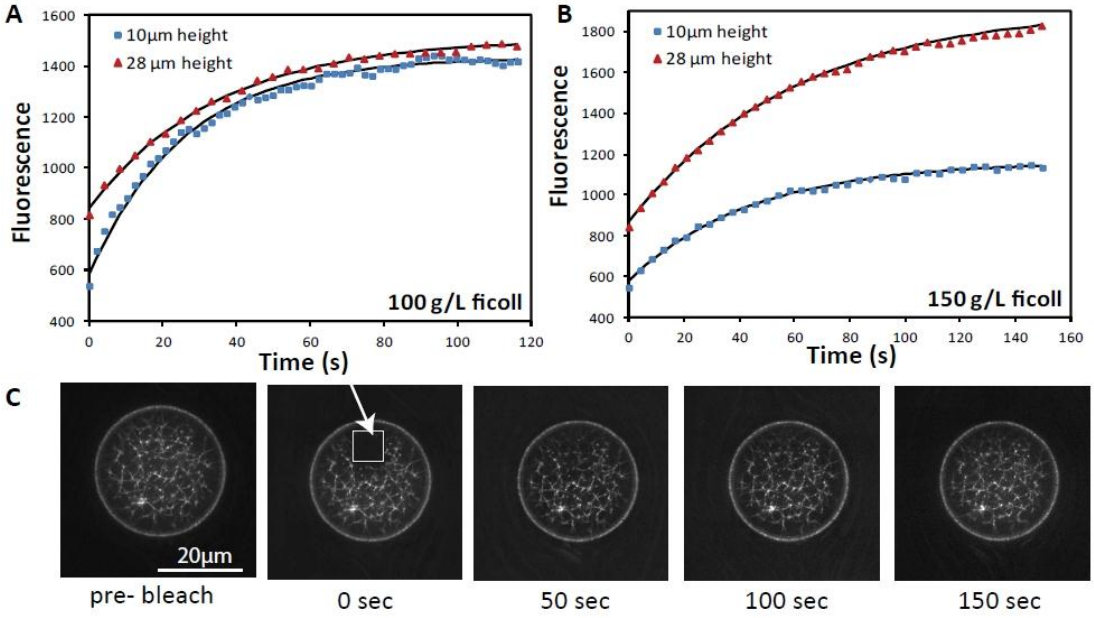

FRAP on FtsZ bundles in spherical and disc-shaped droplets containing the same FtsZ concentration (1 g L^{-1}). The fluorescence intensity of the photobleached region was measured over time in droplets containing (A) 100g L^{-1} Ficoll and (B) 150g L^{-1} Ficoll. For 100 g L^{-1} Ficoll, the half time recovery was 25 s in spherical droplets and 20 s in disc-shaped droplets. For 150 g L^{-1} Ficoll, the half time recovery was 38 s in spherical droplets and 29 s in disc-shaped droplets (C) Time-lapse series of fluorescence images showing the time course of fluorescence recovery. The white arrow shows the bleached region.

Figure S6. Arrangement of FtsZ bundles in droplets containing 150 g/L Ficoll and different FtsZ concentrations

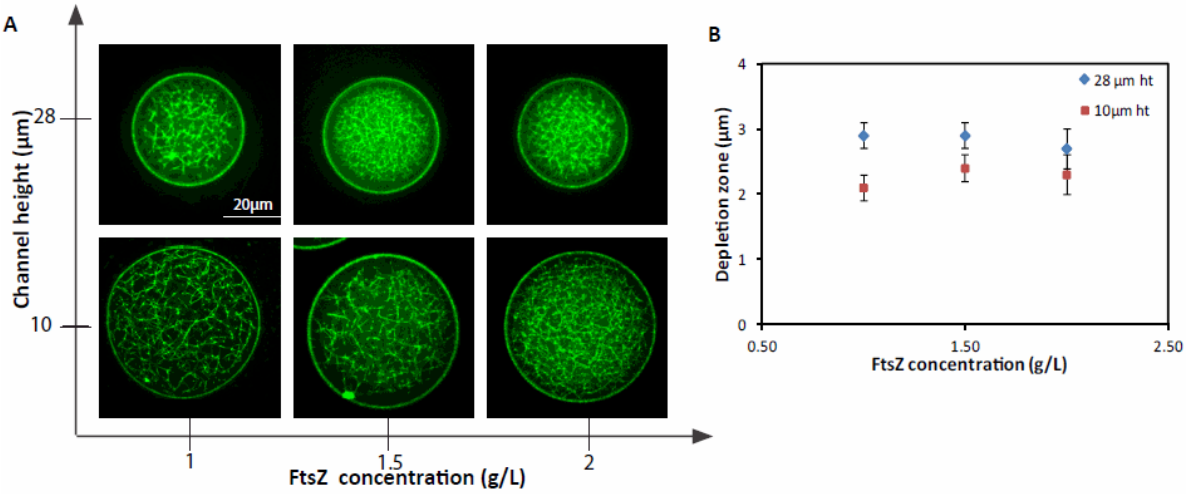

Variation on FtsZ bundles distribution with protein concentration in the presence of 150 g L^{-1} Ficoll 70. (A) Representative confocal images of spherical and disc-shaped droplets. (B) Width of the depletion zone versus FtsZ. Error bars represent the standard deviation of the mean. The bundle density and thickness increased with the FtsZ concentration, while the depletion zone is roughly constant for the spherical (2.8 µm ± 0.1 µm) and for the disc-shaped droplets (2.3 ± 0.2 µm). It seems that with a higher Ficoll 70 concentration, the FtsZ bundle structure is more rigid and independent of the FtsZ concentration.